



**HAL**  
open science

## Targeting chalcone binding sites in living *Leishmania* using a reversible fluorogenic benzochalcone probe

Ariane Batista, Suellen Oliveira, Sébastien Pomel, Pierre-Henri Commere, Valérie Mazan, Moses Lee, Philippe Loiseau, Bartira Rossi-Bergmann, Eric Prina, Romain Duval

### ► To cite this version:

Ariane Batista, Suellen Oliveira, Sébastien Pomel, Pierre-Henri Commere, Valérie Mazan, et al.. Targeting chalcone binding sites in living *Leishmania* using a reversible fluorogenic benzochalcone probe. *Biomedicine and Pharmacotherapy*, 2022, 149, pp.112784. 10.1016/j.biopha.2022.112784 . pasteur-03692205

**HAL Id: pasteur-03692205**

**<https://pasteur.hal.science/pasteur-03692205>**

Submitted on 9 Jun 2022

**HAL** is a multi-disciplinary open access archive for the deposit and dissemination of scientific research documents, whether they are published or not. The documents may come from teaching and research institutions in France or abroad, or from public or private research centers.

L'archive ouverte pluridisciplinaire **HAL**, est destinée au dépôt et à la diffusion de documents scientifiques de niveau recherche, publiés ou non, émanant des établissements d'enseignement et de recherche français ou étrangers, des laboratoires publics ou privés.



Distributed under a Creative Commons Attribution - NonCommercial - NoDerivatives 4.0 International License



## Targeting chalcone binding sites in living *Leishmania* using a reversible fluorogenic benzochalcone probe

Ariane S. Batista<sup>a,1</sup>, Suellen D.S. Oliveira<sup>b,1</sup>, Sébastien Pomel<sup>c</sup>, Pierre-Henri Commere<sup>d</sup>, Valérie Mazan<sup>e</sup>, Moses Lee<sup>f</sup>, Philippe M. Loiseau<sup>c</sup>, Bartira Rossi-Bergmann<sup>g</sup>, Eric Prina<sup>h</sup>, Romain Duval<sup>i,\*</sup>

<sup>a</sup> Nanotechnology Engineering Program, Instituto Alberto Luiz Coimbra de Pós-Graduação e Pesquisa de Engenharia - COPPE, Universidade Federal do Rio de Janeiro, Rio de Janeiro, 21941-972, Brazil

<sup>b</sup> Department of Anesthesiology, University of Illinois, Chicago 60612, USA

<sup>c</sup> Université Paris-Saclay, CNRS, BioCIS, 92296 Châtenay-Malabry, France

<sup>d</sup> Plateforme de Cytométrie, Institut Pasteur, 75015 Paris, France

<sup>e</sup> Université de Strasbourg, Université de Haute-Alsace, CNRS, LIMA, UMR 7042, ECPM, 25 Rue Becquerel, 67000 Strasbourg, France

<sup>f</sup> Department of Chemistry, Georgia State University, Atlanta 30303, USA

<sup>g</sup> Instituto de Biofísica Carlos Chagas Filho, Universidade Federal de Rio de Janeiro, 21941-902 Rio de Janeiro, Brazil

<sup>h</sup> Institut Pasteur, Unité de Parasitologie Moléculaire et Signalisation, INSERM U1201, Paris, France

<sup>i</sup> Université de Paris, IRD, MERIT, F-75006 Paris, France

### ARTICLE INFO

#### Keywords:

Chalcones  
*Leishmania amazonensis*  
Fluorescence  
Cell imaging  
Cytometry  
Pharmacology

### ABSTRACT

Chalcones (1,3-diphenyl-2-propen-1-ones) either natural or synthetic have a plethora of biological properties including antileishmanial activities, but their development as drugs is hampered by their largely unknown mechanisms of action. We demonstrate herein that our previously described benzochalcone fluorogenic probe (**HAB**) could be imaged by fluorescence microscopy in live *Leishmania amazonensis* promastigotes where it targeted the parasite acidocalcisomes, lysosomes and the mitochondrion. As in the live zebrafish model, **HAB** formed yellow-emitting fluorescent complexes when associated with biological targets in *Leishmania*. Further, we used **HAB** as a reversible probe to study the binding of a portfolio of diverse chalcones and analogues in live promastigotes, using a combination of competitive flow cytometry analysis and cell microscopy. This pharmacological evaluation suggested that the binding of **HAB** in promastigotes was representative of chalcone pharmacology in *Leishmania*, with certain exogenous chalcones exhibiting competitive inhibition (ca. 20–30%) towards **HAB** whereas non-chalconic inhibitors showed weak capacity (ca. 3–5%) to block the probe intracellular binding. However, this methodology was restricted by the strong toxicity of several competing chalcones at high concentration, in conjunction with the limited sensitivity of the **HAB** fluorophore. This advocates for further optimization of this indirect target detection strategy using pharmacophore-derived reversible fluorescent probes.

### 1. Introduction

Chalcones (1,3-diphenyl-2-propen-1-ones) of natural or synthetic origin constitute an important class of biologically active compounds (Fig. 1) [1–3]. From a medicinal chemistry standpoint, the chalcone system can be seen as a molecular scaffold allowing the probing of binding sites through iterative pharmacomodulation on the aromatic rings [4]. Chalcones are also considered small-molecule effectors of

cellular functions, being capable as variably reactive electrophiles to modulate or inhibit biological nucleophiles, particularly thiols [1,5–8]. Despite these unique features, many mechanisms of action of chalcones at the cell level remain elusive, with few established protein targets [1–3,6,7,9–11] (Fig. 1) and poor therapeutic deployment up to now [3].

From the intrinsically non-fluorescent chalcone skeleton, we designed and validated a unique fluorogenic benzochalcone congener, 4'-hydroxy-3-aminobenzochalcone (**HAB**, Fig. 2) possessing elevated

\* Corresponding author.

E-mail address: [romain.duval@ird.fr](mailto:romain.duval@ird.fr) (R. Duval).

<sup>1</sup> These authors contributed equally to the present work.

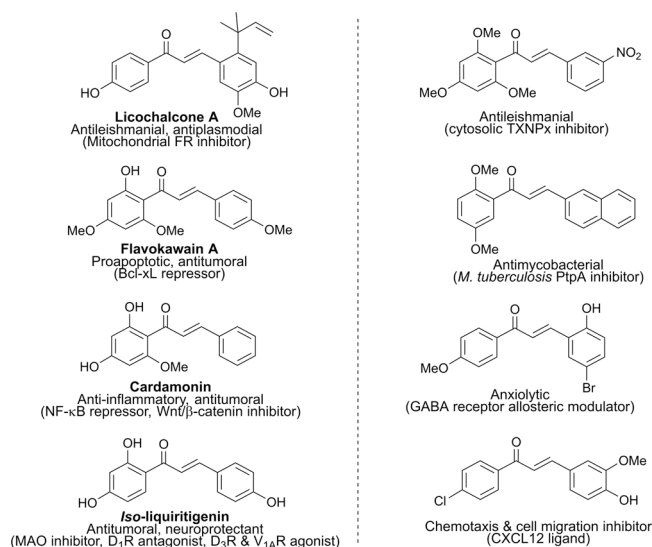


**Fig. 1.** Examples of bioactive chalcones and their identified protein targets / mechanisms of action (*left panel*: natural compounds; *right panel*: synthetic compounds). Bcl-xL, B-cell lymphoma extra-large; DR, dopamine receptor; FR, fumarate reductase; GABA,  $\gamma$ -aminobutyric acid; CXCL, C-X-C lymphokine; MAO, monoamine oxidase; NF, nuclear factor; Ptp, protein tyrosine phosphatase; TXNpx, trypanredoxin peroxidase; VR, vasopressin receptor.

cytopermeability for live-cell and live-animal imaging. **HAB** was found to be a highly specific non-covalent tracer of neutrophil granules in live zebrafish (*Danio rerio*) larva, constituting a novel vital stain to monitor and study neutrophil-dependent events in this animal model [12]. Taking into account the great number of chalcones, either natural or synthetic, that show antileishmanial activity [1,9,13–22], we chose to investigate the behavior of **HAB** in *Leishmania in vitro*.

Our strategy was based on two sequential steps: (i) the identification of **HAB** target organelles in *L. amazonensis* promastigotes by live-cell imaging, and (ii) the use of **HAB** as a platform to evaluate its blockage from binding sites in promastigotes by putative competitors, using a

combination of flow cytometry and microscopic imaging analysis. Importantly, **HAB** is a reversible probe due to its extended conjugation pattern and electron-rich integrated fluorophore [12], making it a very weak electrophile. In comparison, many antileishmanial chalcones behave as electrophilic inhibitors [7], limiting their use as models for fluorescent probes, firstly because of their irreversible binding to nucleophilic targets, secondly due to the predicted ablation of fluorescence properties upon electrophilic trapping. Eleven compounds (cpd.) were selected for the study as potential competitors, consisting of five chalcones (cpd. 1-5) [14,15,18–20] with established antileishmanial activity, together with four chalcones (cpds. 6-9) [12,23,24] and two non-chalconic analogues (cpds. 10-11) [23,25] not previously investigated as antileishmanials (Fig. 2). This competition approach aimed to provide with an indirect means of identifying the target organelles of relevant antileishmanial compounds, corresponding to a critical step in their drug development [1,7,9,22]. So far, unravelling chalcone targets in *Leishmania* has proven difficult [1,7,9,13,22] despite their possible similarity with established targets in better-studied systems (e. g., heat-shock proteins in cancer cells) [26,27], which could guide the former investigation.

## 2. Experimental section

Dulbecco's modified Eagle medium (DMEM), medium 199 and fetal calf serum (FCS) were obtained from Cultilab. Poly-L-lysine was purchased from Sigma-Aldrich. LTR® was purchased from Invitrogen. Technical MitoRed was purchased from Sigma-Aldrich, and purified by chromatography (silica gel 60 Merck, *i*-PrOH 100%) before use. DAPI staining was performed using Vectashield® (Vector Lab. Inc). 7-Amino-actinomycin D (7-AAD) was from Affymetrix-eBiosciences. *Iso*-cardamonin (2',4'-dihydroxy-6'-methoxychalcone) **1** was isolated from *Piper aduncum* as described previously [14]. Flavokawain A **2** (4-methoxy-2'-hydroxy-4',6'-dimethoxychalcone), chalcone **3** and chalcone **6** were prepared in one step by Claisen-Schmidt condensation as previously described [18]. Chalcones **4**, **5** [19] and **7** [19] were provided by Prof. Guy Lewin (Laboratoire de Pharmacognosie, UMR 8076 BioCIS CNRS, Châtenay-Malabry, France). **HAB**, benzochalcones **8** and **9**, pyrazole **10** and enone **11** were previously described by the authors [12,

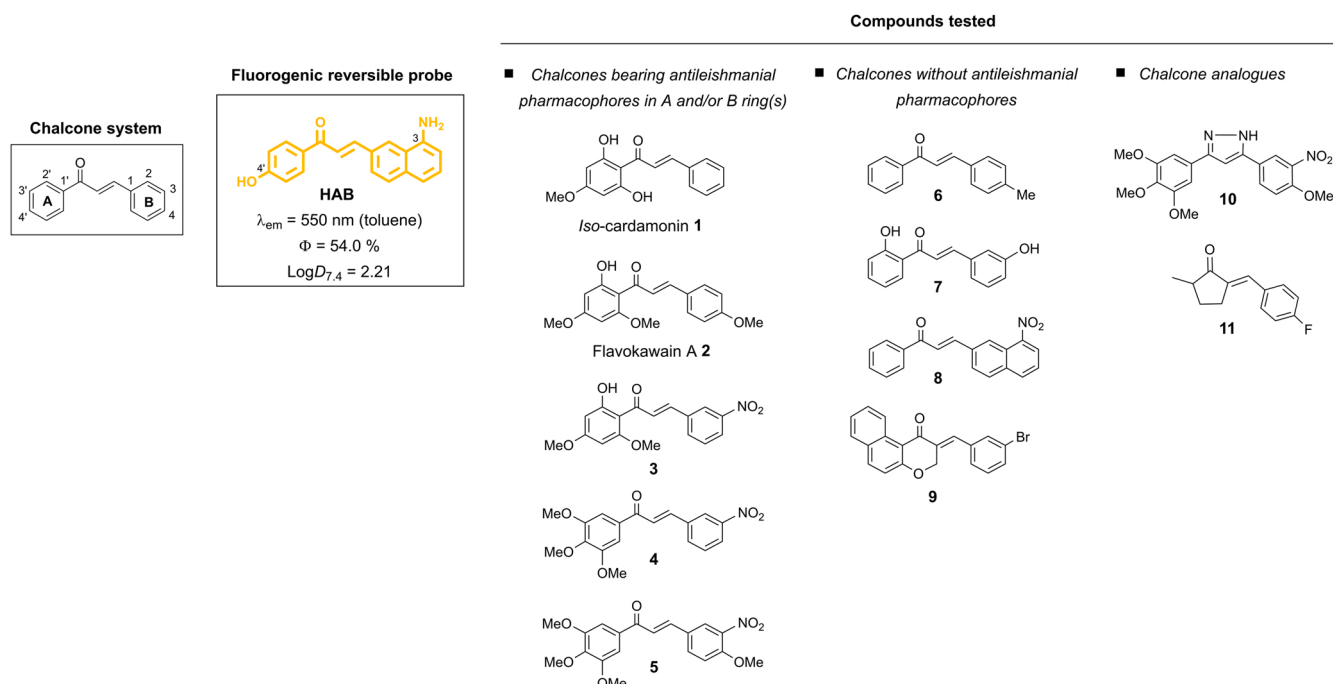


**Fig. 2.** Chemical structures of the reversible fluorogenic probe **HAB** and of selected putative competitors for cell-based studies.

23–25]. All compounds showed high purity (>97%) by  $^1\text{H}$  and  $^{13}\text{C}$  NMR, elemental analysis and HRMS. Live-cell imaging of Balb/c mouse macrophages and MHOM/BR/75/Josefa strain of *L. amazonensis* promastigotes was performed using an Axiovert 200 M Zeiss microscope equipped with ApoTome system, using the following settings: DAPI,  $\lambda_{\text{ex}} = 359\text{--}371\text{ nm}$ ,  $\lambda_{\text{em}} = 397\text{ nm}$ ; **HAB**,  $\lambda_{\text{ex}} = 450\text{--}490\text{ nm}$ ,  $\lambda_{\text{em}} = 515\text{--}565\text{ nm}$ ; LTR® and MitoRed,  $\lambda_{\text{ex}} = 540\text{--}552\text{ nm}$ ,  $\lambda_{\text{em}} = 575\text{--}640\text{ nm}$ . Live-cell flow cytometry was performed on a Gallios flux cytometer from Beckman-Coulter (Villepinte, France) using the following settings: FL4 (7-AAD),  $\lambda_{\text{ex}} = 488\text{ nm}$ ,  $\lambda_{\text{em}} = 650\text{--}695\text{ nm}$ ; FL10 (**HAB**),  $\lambda_{\text{ex}} = 405\text{ nm}$ ,  $\lambda_{\text{em}} = 540\text{--}550\text{ nm}$ .

### 2.1. Culture of *L. amazonensis* promastigotes.

*L. amazonensis* promastigotes (MHOM/BR/75/Josefa strain) were kept in culture flasks at 26 °C in medium 199 containing penicillin (50 UI/mL) and streptomycin (50 µg/mL), and supplemented with sterile human urine (2%), haem (5 µg/mL) and CFS (10%). The working promastigote suspension was adjusted to 20,000 cells/µL before use.

### 2.2. Co-localization experiments in live *L. amazonensis* promastigotes

98 µL of promastigote suspension were transferred to an Eppendorf tube and treated sequentially with: (a) LTR® (10 µM in DMSO, 1 µL, 100 nM in medium) or MitoRed (5 µM in DMSO, 1 µL, 50 nM in medium) and incubated for 20 min at 18 °C; (b) **HAB** (0.5 mM in DMSO, 1 µL, 5 µM in medium) and incubated for 10 min at 20 °C. Homogenizing was done after each addition by vortexing cells for 3 s. 7 µL of promastigote suspension were deposited on a glass coverslip coated with poly-L-lysine and the coverslip was mounted on a glass slide. Cells were allowed to adhere in an inverted position for 30 min on an ice-cold metal plate before microscopic observation was performed. All experiments were done in triplicates.

### 2.3. In vitro inhibitory activity

Evaluation of the *in vitro* antipromastigote activity of **HAB** and chalcone competitors was performed in 96-well tissue culture plates in a final volume of 200 µL containing ca.  $4 \times 10^5$  promastigotes per well. Inhibitors were subjected to a two-fold serial dilution in triplicate. The antileishmanial drug used as positive control was amphotericin B (Amp B). The parasites were cultivated for 72 hrs at 26 °C in a 5% CO<sub>2</sub> atmosphere. Cell viability was analyzed with a colorimetric assay using 3-(4,5-dimethylthiazol-2-yl)-2,5-diphenyl tetrazolium bromide (MTT). Mean IC<sub>50</sub> were determined by linear regression analysis and expressed in µM ± SD [28].

### 2.4. Cytometric quantification of **HAB** blockage by competitors in live *L. amazonensis* promastigotes

465 µL of promastigote suspension were transferred to a plastic test tube and treated sequentially at 20 °C with: (a) competitor (10 mM in DMSO, 5 µL, 100 µM in medium) and incubated for 30 min; (b) **HAB** (0.5 mM in DMSO, 5 µL, 5 µM in medium) and incubated for 10 min; (c) 7-AAD (50 µg/mL in PBS, 25 µL, 40 µM in medium) and incubated for 30 min before flow cytometry analysis was performed. All experiments were done in triplicates.

### 2.5. Microscopic competition analysis in live *L. amazonensis* promastigotes

97 µL of promastigote suspension were transferred to an eppendorf tube and treated sequentially at 20 °C with: (a) LTR® (10 µM in DMSO, 1 µL, 100 nM in medium) or MitoRed (5 µM in DMSO, 1 µL, 50 nM in medium) and incubated for 20 min; (b) competitor (10 mM in DMSO, 1 µL, 100 µM in medium) and incubated for 30 min; (c) **HAB** (0.5 mM in

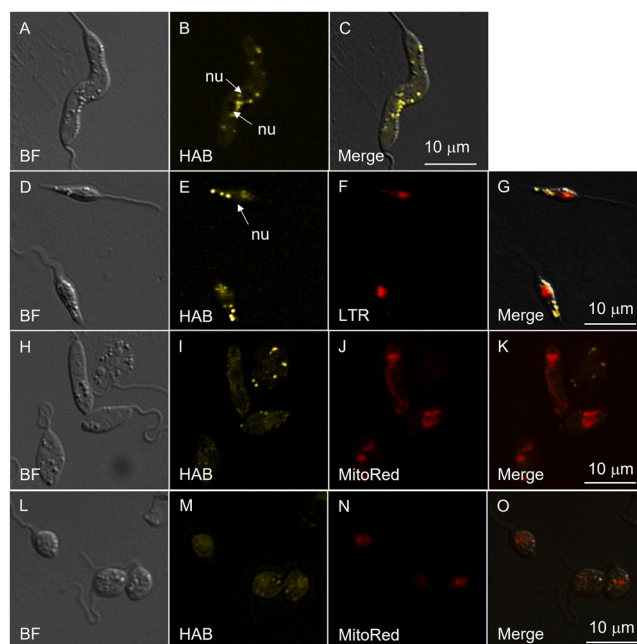


**Fig. 3.** Microscopic fluorescence imaging of **HAB** (5 µM) in *L. amazonensis* promastigotes in presence of LTR (100 nM) or MitoRed (50 nM). A, D, H, L: bright field imaging; B, E, I, M: **HAB** labelling; F: LTR labelling; J, N: MitoRed labelling; C, G, K, O: merge. Abbreviations used: nu, nucleus; BF, bright field. The images are representative of three independent experiments.

DMSO, 1 µL, 5 µM in medium) and incubated for 10 min. Homogenizing was done after each addition by vortexing cells for 3 s. Microscopic observation was performed in triplicates as described previously.

## 3. Results and discussion

### 3.1. In vitro imaging study in *L. amazonensis* promastigotes

When incubated at 5 µM, **HAB** was rapidly incorporated by live *L. amazonensis* promastigotes and distributed heterogeneously within the intracellular space (Fig. 3). **HAB** was found to label the acidocalcisomes (ACC), small acidic vesicular organelles specific to trypanosomatid parasites, and known to most often cluster at the posterior end of promastigotes [29–31]. Co-localization of **HAB** with anti-vacuolar-type proton pyrophosphatase antibodies specific to the ACC [31,32] failed due to loss of **HAB** signals upon fixation [12], whereas the classical ACC dye acridine orange [32–34] showed spectral overlap with **HAB** (data not shown). However, we took advantage of the unique feature of ACC to be visualized in bright-field microscopy in the absence of any tracer [31] to determine ACC and **HAB** co-localization (Fig. 3A–C, D–E and H–I). **HAB** also labelled the promastigote multi-vesicular early lysosomes, typically located next to the flagellar pocket at the anterior end of the cell body [29,30,35], as demonstrated by its co-localization with the acidotropic dye LysoTrackerRed® (LTR) (Fig. 3E–G). While LTR labelling is pharmacologically non-specific (*i. e.*, sequestration of the protonated amine dye within acidic organelles), a target-mediated labelling of the ACC and lysosomes by **HAB** was invoked in promastigotes because of its very weak basicity (predicted pKa value of 3.97 for the **HAB** amino tautomers) [12], which is ca.  $10^5$  lower than that of lysosomotropic amines (pKa values of 9–9.5). To prove this hypothesis, the acido-basic properties of **HAB** were measured in pure water to address physiological relevance. However, precise determination of pKa values was hindered by the limited aqueous solubility of **HAB** under its neutral form with formation of colloids (Fig. S1, Supporting Information). Using a methanol/water system (80:20 w/w) allowed to record **HAB** UV–vis absorption spectra within a large pH

**Table 1**

Biological evaluation of chalcones 1-9<sup>[a]</sup> and analogues 10-11<sup>[a]</sup> as anti-leishmanials<sup>[b]</sup> and **HAB**<sup>[c]</sup> competitors in live *L. amazonensis* promastigotes<sup>[d]</sup>.

Cpd.	IC <sub>50</sub> ( $\mu$ M) <sup>[b]</sup>	Mean survival by FACS <sup>[e]</sup> (%)	Mean fluorescence intensity (a. u.)	Mean blockage normalized on survival <sup>[f]</sup> (%)	Cell population representativity
<b>HAB</b>	3.57	100	2.68 $\pm$ 0.13	NA	Good
1	0.32 $\pm$ 0.13	97.6 $\pm$ 3.3	2.02 $\pm$ 0.15	22.8	Good
2	7.60 $\pm$ 0.61	18.5 $\pm$ 1.5	1.74 $\pm$ 0.28	< 0	Poor
3	0.45 $\pm$ 0.01	18.0 $\pm$ 3.7	1.48 $\pm$ 0.04	< 0	Poor
4	0.26 $\pm$ 0.0025	91.5 $\pm$ 2.6	1.75 $\pm$ 0.21	28.6	Good
5	2.46 $\pm$ 0.20	29.3 $\pm$ 2.9	2.29 $\pm$ 0.27	< 0	Poor
6	14.34 $\pm$ 4.06	93.4 $\pm$ 8.2	1.94 $\pm$ 0.40	22.5	Good
7	0.83 $\pm$ 0.22	98.6 $\pm$ 11.0	2.10 $\pm$ 0.09	20.5	Good
8	1.74 $\pm$ 0.14	57.3 $\pm$ 4.2	1.89 $\pm$ 0.17	< 0	Poor
9	4.08 $\pm$ 0.49	40.8 $\pm$ 2.2	1.46 $\pm$ 0.09	< 0	Poor
10	> 50	91.3 $\pm$ 7.6	2.37 $\pm$ 0.19	3.1	Good
11	8.59 $\pm$ 1.03	95.4 $\pm$ 4.5	2.44 $\pm$ 0.05	4.6	Good
Amp B	0.05 $\pm$ 0.0073	7.0 $\pm$ 1.3	NA	NA	Good

[a] Incubated at 100  $\mu$ M in cytometric and imaging experiments. [b] Results obtained in MTT assays assessing the inhibition of parasite proliferation [28]. [c] Incubated at 5  $\mu$ M in cytometric and imaging experiments. [d] All results were obtained from triplicates. [e] Mean survival was normalized on survival in presence of 5  $\mu$ M **HAB**, which was 102.3  $\pm$  8.1% relatively to control (DMSO). [f] Mean blockage normalized on survival was calculated using the formula: [(mean fluorescence intensity of **HAB** alone - mean fluorescence intensity of **HAB** in presence of competitor) / mean fluorescence intensity of **HAB** alone] x (100 / % survival in presence of competitor). Amp B: amphotericin B (incubated at 2  $\mu$ M in cytometric experiments); a. u., arbitrary units; N. A.: non-applicable.

range (Fig. S2, Supporting Information). Data processing led to experimental pK<sub>a</sub> values of 2.9 (amine function) and 9.3 (phenol function) in this system, demonstrating the full neutrality of **HAB** across a wide range of physiological pH (Fig. S3, Supporting Information). Consequently, these results exclude any passive acidotropic trapping of **HAB** into the ACC and lysosomes (intra-organelle pH values of 4.5–5) [36, 37]. Unexpectedly, ACC were consistently LTR-negative under our conditions (a faint ACC labelling by LTR can be seen in Fig. 3F. See also Figs. 5–7 for LTR-negative ACC). This observation can be rationalized by the fact that the acidity of the ACC dramatically depends on culture conditions, and can be low in satiated, healthy parasites [33,34,38,39].

Additionally, **HAB** was found to label the large parasite mitochondrion as demonstrated by co-localization with the specific tracker MitoRed [40–42] (Fig. 3I–K). A similar mitochondrial labelling was observed in stressed promastigotes displaying a round morphology [43, 44] (Fig. 3M–O), suggesting that the penetration of **HAB** in the parasite mitochondria was independent of its inner membrane potential. Importantly, the affinity of **HAB** for the mitochondria appeared to be promastigote-specific, since labelling was absent from the mitochondria of zebrafish larva neutrophils [12] and mouse peritoneal macrophages (Fig. S7, Supporting Information). **HAB** did not appear to label the nucleus (Fig. 3B and E). A general lack of nuclear tropism for **HAB** is further supported by the absence of **HAB** labelling in DAPI-stained macrophage nuclei (Figs. S7 and S8, Supporting information). While the parasite mitochondrion is an established [1,9,13] or suspected [7,

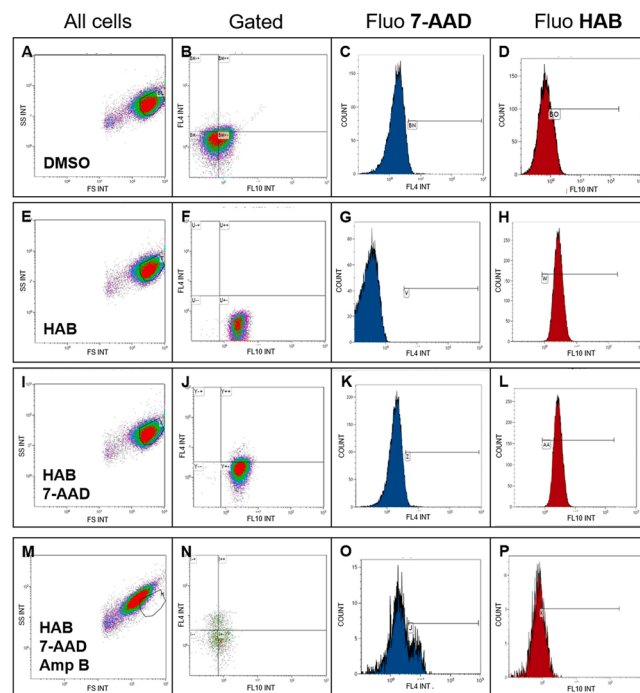


**Fig. 4.** Cytometric quantification of **HAB** (5  $\mu$ M) in live *L. amazonensis* promastigotes (20,000 cells/ $\mu$ L) in presence of 7-AAD (20  $\mu$ M) and presence / absence of Amp B (2  $\mu$ M). A, E, I and M: morphological biparametric plots (FS, cell size; SS, cell granularity); B, F, J and N: gated plots (FL4: 7-AAD, FL10: **HAB**); C, G, K and O: 7-AAD cytometric histograms; D, H, L and P: **HAB** cytometric histograms. Plot data are representative of three independent experiments. Means and standard deviations of cell count and fluorescence intensity data (n = 3) are indicated in Table 1.

45–47] target organelle of antileishmanial chalcones, the ACC and lysosomes are herein identified for the first time as harboring chalcone-binding sites.

### 3.2. In vitro pharmacological study in *L. amazonensis* promastigotes

Having identified the subcellular tropism of **HAB** in promastigotes, we assessed its pharmacological value as a reversible probe in competitive flow cytometry and cell imaging experiments. Pharmacological specificity of given bioactive molecules is classically established by their displacement or blockage of a reference compound (generally a radioligand or a fluorescently labelled derivative) [48]. We used here putative **HAB** competitive inhibitors under the form of chalcones or analogues, to quantify their ability to specifically block **HAB** from accessing its subcellular binding sites, delineating the presence of action sites for these competitors in promastigotes. Due to the pronounced solvatochromism of **HAB** [12], its binding inhibition by effective competitors would result in **HAB** remaining free (i. e. protein-unbound) in the cytosol, with a fluorescence known to be negligible [12]. The obtained signals would hence be reported to that of protein-bound **HAB** in absence of any competitor. The eleven putative competitors 1-11 were initially evaluated *in vitro* against *L. amazonensis* promastigotes for antileishmanial activity [28], providing with a spectrum of activity in the micromolar range with several potent inhibitors, in accordance with literature data (Table 1). All competitors were also checked for their complete absence of fluorescence at the concentration used in the competition assay, which was set to a twenty-fold ratio (100  $\mu$ M) respective to **HAB** (5  $\mu$ M). Parasite viability was assessed in presence of competitors using the membrane impermeant dye 7-aminoactinomycin D (7-AAD) at 20  $\mu$ M, a cytometric marker of compromised cells [49] chosen for non-overlapping spectrally with **HAB** (Figs. 4–7). **HAB** itself was deprived of short-term toxicity at 5  $\mu$ M (100% cell viability after

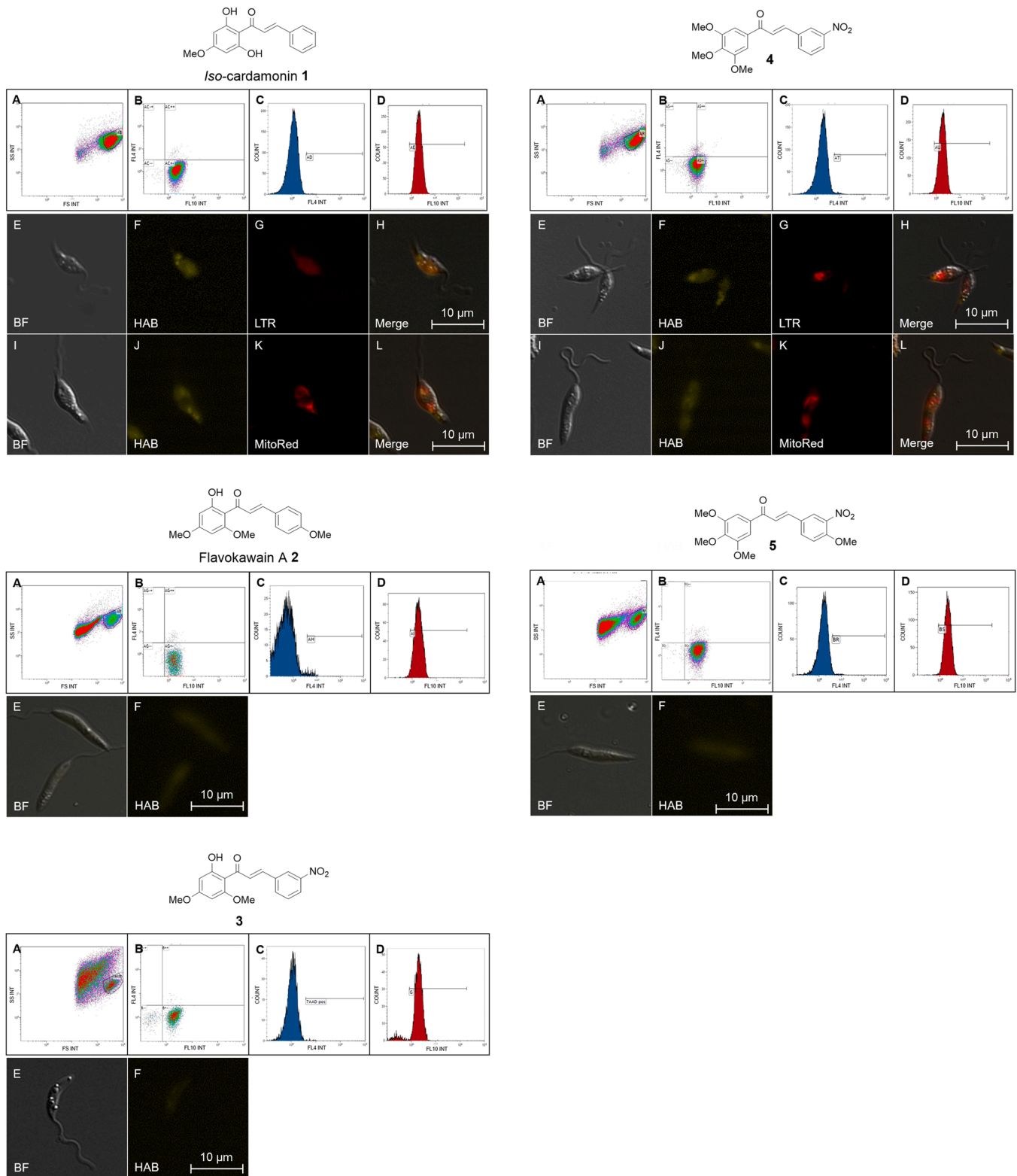


**Fig. 5.** Cytometric quantification and microscopic fluorescence imaging of **HAB** (5  $\mu$ M) in live *L. amazonensis* promastigotes (20,000 cells/ $\mu$ L) in presence of competitors 1-5 (100  $\mu$ M). Co-markers were 7-AAD (40  $\mu$ M), LTR (100 nM) or MitoRed (50 nM). A: morphological biparametric plot (FS, cell size; SS, cell granularity); B: gated plot (FL4: 7-AAD, FL10: **HAB**); C: 7-AAD cytometric histogram; D: **HAB** cytometric histogram; E and I: bright field (BF); F and J: **HAB** labelling; G: LTR labelling; K: MitoRed labelling, H and L: merge. IC<sub>50</sub> values of competitors 1-5 are given in [Table 1](#). Plot data are representative of three independent experiments. Means and standard deviations of cell count and fluorescence intensity data (n = 3) are indicated in [Table 1](#).

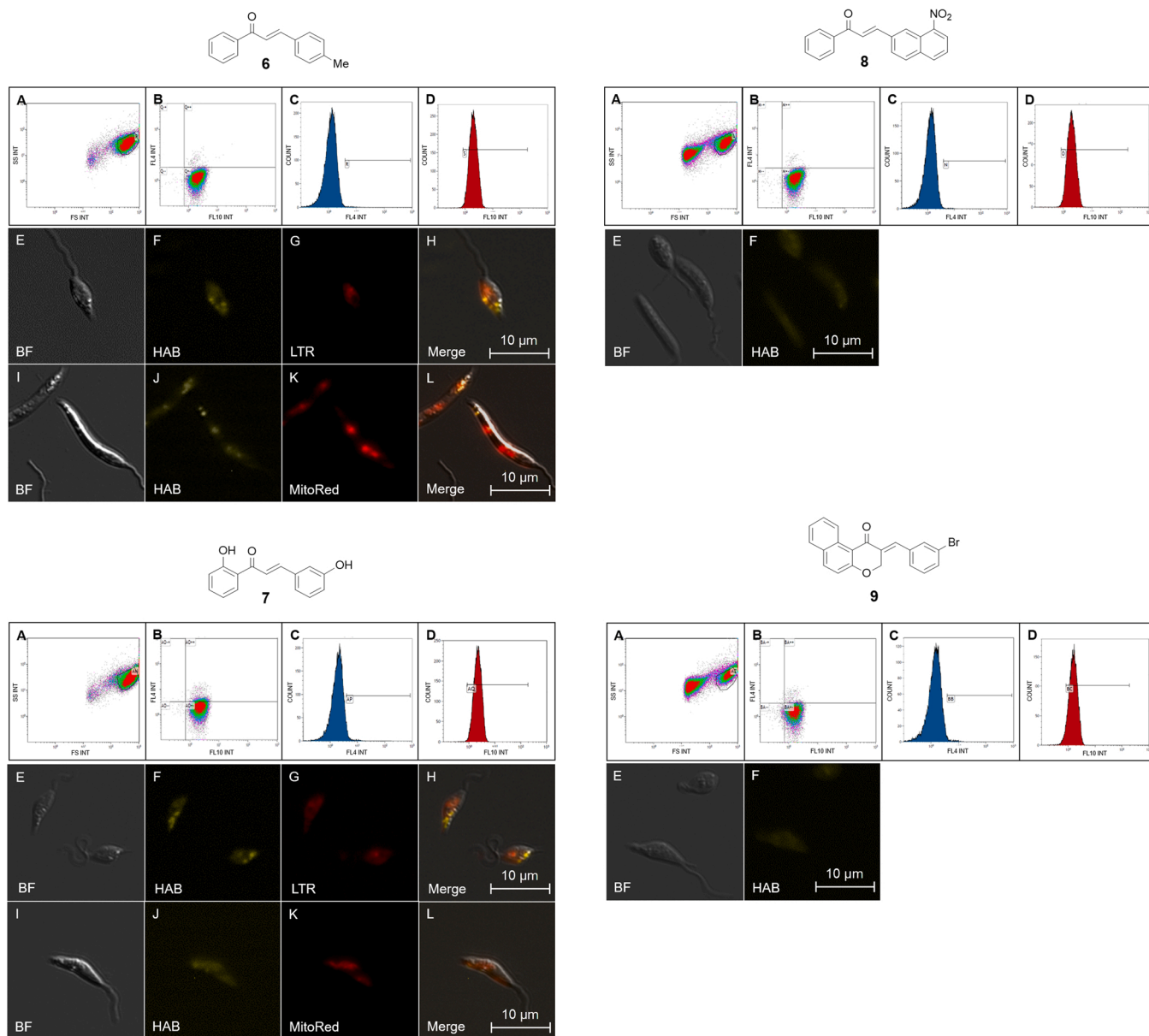


**Fig. 6.** Cytometric quantification and microscopic fluorescence imaging of HAB (5 μM) in live *L. amazonensis* promastigotes (20,000 cells/μL) in presence of competitors 6-9 (100 μM). Co-markers were 7-AAD (40 μM), LTR (100 nM) or MitoRed (50 nM). A: morphological biparametric plot (FS, cell size; SS, cell granularity); B: gated plot (FL4: 7-AAD, FL10: HAB); C: 7-AAD cytometric histogram; D: HAB cytometric histogram; E and I: bright field (BF); F and J: HAB labelling; G: LTR labelling; K: MitoRed labelling, H and L: merge. IC<sub>50</sub> values of competitors 6-9 are given in Table 1. Plot data are representative of three independent experiments. Means and standard deviations of cell count and fluorescence intensity data (n = 3) are indicated in Table 1.

40 min), whereas the effect of complete cell viability loss was assessed with Amp B at 2 μM (Fig. 4). Competition experiments were performed by treating live *L. amazonensis* promastigotes with putative competitors for 30 min, staining with HAB for 10 min then 7-AAD for 30 min prior to flow cytometry analysis (Figs. 5–7).

We firstly investigated the established antileishmanial chalcones 1-5, possessing pharmacophores at the A and/or B rings. In this group, 3-nitrochalcone 3 corresponds to a desmethoxy analogue of the recently described inhibitor of cytosolic trypanothione peroxidase in various *Leishmania* species (Fig. 1), of which it constitutes the lead precursor [7]. Amongst these antileishmanials, the moderate natural inhibitor isocardamonin 1 from *Piper aduncum* [14,15,18] and the potent synthetic 3-nitrochalcone 4 [19] did not exhibit short-term toxicity (cell viability > 90% after 70 min), and induced significant (23–29%) competitive blockage of HAB in promastigotes (Fig. 5 and Table 1). On the other hand, natural flavokawain A 2 from *Piper methysticum* [18,20,50] and

3-nitrochalcone 3 [18], possessing a common xanthoxyline-derived pharmacophore as ring A, were highly cytotoxic at 100 μM (18% residual cell viability after 70 min), inducing cell membrane disruption as indicated by morphological cytometric plots (Fig. 5). This effect precluded normalization of their exerted competitive blockage in the non-representative populations of surviving cell (Table 1). The same phenomenon occurred with chalcone 5, a 4-methoxylated derivative of 3-nitrochalcone 4 [19], which led to a low cell survival of ca. 30% (Fig. 5 and Table 1). Noteworthy, cell lysis at 100 μM in presence of chalcones 1–5 was not correlated with the presence or absence of pharmacophoric moiety (e. g., the 3',4',5'-trimethoxyphenyl ring A common to competitors 4 and 5) nor with IC<sub>50</sub> values (Fig. 5 and Table 1). Despite the cytometric measurement of significant blockage of HAB by isocardamonin 1 and chalcone 4, this phenomenon could not be correlated microscopically with objective changes of HAB fluorescence at the level of labeled organelles (i. e. ACC, lysosomes or mitochondrion) in

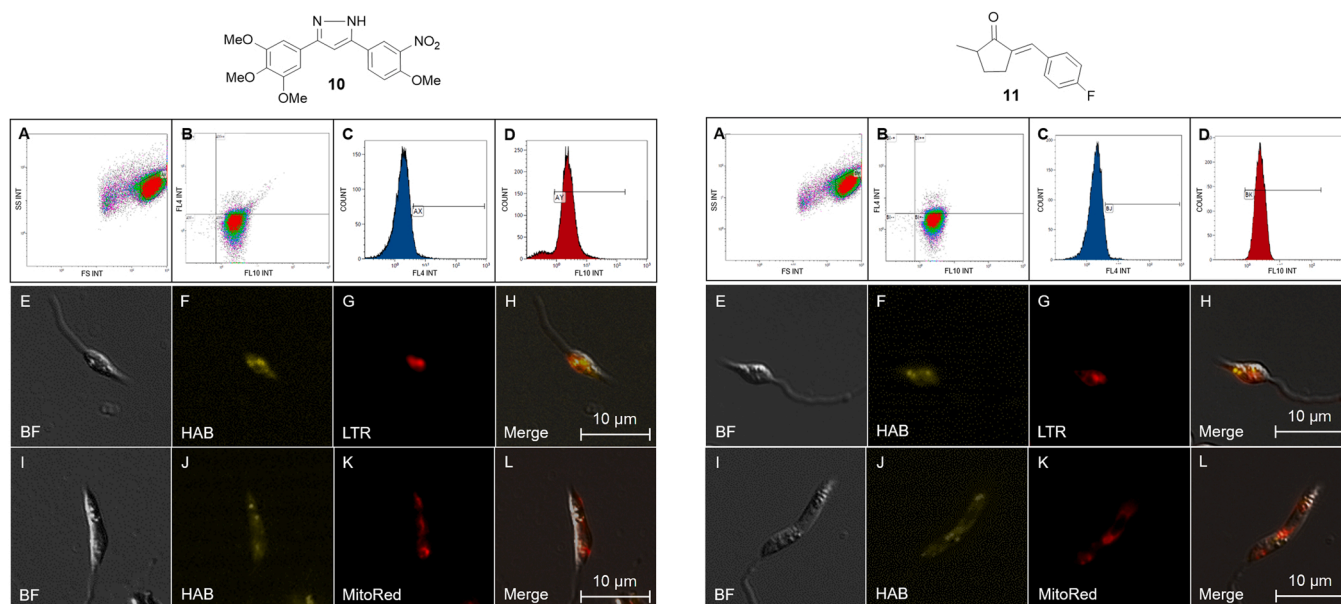


**Fig. 7.** Cytometric quantification and microscopic fluorescence imaging of **HAB** (5  $\mu$ M) in live *L. amazonensis* promastigotes (20,000 cells/ $\mu$ L) in presence of competitors **10-11** (100  $\mu$ M). Co-markers were 7-AAD (40  $\mu$ M), LTR (100 nM) or MitoRed (50 nM). A: morphological biparametric plot (FS, cell size; SS, cell granularity); B: gated plot (FL4: 7-AAD, FL10: **HAB**); C: 7-AAD cytometric histogram; D: **HAB** cytometric histogram; E and I: bright field (BF); F and J: **HAB** labelling; G: LTR labelling; K: MitoRed labelling, H and L: Merge. IC<sub>50</sub> values of competitors **10-11** are given in [Table 1](#). The results were done in triplicates (cytometric means and standard deviations are given in [Table 1](#)) and are representative of three independent experiments.

promastigotes ([Fig. 5](#)). This fact may be explained by the rather modest competitions exerted (< 30%). Regarding **HAB** labeling in promastigotes surviving 100  $\mu$ M of flavokawain **A 2**, chalcone **3** or chalcone **5**, their intracellular fluorescence appeared low and diffuse with absence of detectable subcellular structures ([Fig. 5](#)), although these cells were not displaying an apparent stressed-out phenotype [[43,44](#)] ([Figs. 3 and 5](#)).

Among chalcones lacking known antileishmanial pharmacophores, chalcones **6-9** were yet found to exhibit moderate to good growth inhibitory activities against *L. amazonensis* promastigotes ([Table 1](#)). 4-Methylchalcone **6** and 2',3-dihydroxychalcone **7** were deprived of short-term toxicity at 100  $\mu$ M (cell viability >93% after 70 min) and significantly competed with **HAB** to a similar extend (20–22%), despite their great difference in inhibitory activity ([Fig. 6 and Table 1](#)). On the other hand, benzochalcones **8** [[12](#)] and **9** [[24](#)] induced severe cytotoxicity at 100  $\mu$ M (40–60% residual cell viability after 70 min), impeding normalization of **HAB** blockage ([Fig. 6 and Table 1](#)). Chalcones **6** and **7** did not induce any objective decrease of **HAB** fluorescence within promastigotes by microscopic imaging ([Fig. 6](#)), consistent with the modest competitions exerted. On the other hand, the acutely toxic competitors **8** and **9** were responsible for a similar lack of detectable fluorescence within surviving cells ([Fig. 6](#)).

Moving to non-chalconic analogues, pyrazole **10** and enone **11** [[23, 25](#)] were devoid of short-term toxicity at 100  $\mu$ M (cell viability >91% after 70 min) and induced weak (3–5%) competitive blockage of **HAB** ([Fig. 7 and Table 1](#)). Interestingly, pyrazole **10** corresponds to a cyclized version of chalcone **5** and was found to be more than 20-fold less inhibitory than **5** in proliferation assays, while also being virtually non-toxic at 100  $\mu$ M ([Table 1](#)).

The semi-quantitative profiling obtained using **HAB** as a reversible fluorogenic probe in *L. amazonensis* promastigotes in presence of competitors can be summarized as follows ([Table 1](#)): (a) **HAB** was effective in assessing the binding of all non-toxic competitors. On one hand, among these, chalcones **1, 4, 6** and **7** were responsible for significant competitions which were up to 29% for the potent antileishmanial 3-nitrochalcone **4**. On the other hand, chalcone analogues **10** and **11** appeared to be weak competitors (3–5%) despite growth inhibitory activities in the same range (e. g., enone **11**) than effective chalcones (e. g.,

chalcones **1** and **6**). A chalcone specificity trend for **HAB** is supported by the comparison between chalcone **4** (inducing ca. 29% competitive blockage) and its close congener pyrazole **10** (inducing ca. 3% competitive blockage). However, this trend would need validation, typically by testing a larger set of competitors; (b) a general lack of correlation between IC<sub>50</sub> values, short-term toxicity and competitive potency was observed for all tested compounds. This can be rationalized by the distinctive experimental settings taking place (i. e., cumulative antiproliferative effects over 72 h for parasite growth inhibition assays vs rapid effects after 70 min in flow cytometry experiments), and the various physicochemical features of the tested competitors (i. e., logD values) directly impacting their cell permeability kinetics and effects. It is important to keep in mind that certain chalcones and analogues tested in this study are known to possess weak (i. e., *iso*-cardamonin **1**, 3-nitrochalcone **3**, 3',4',5'-trimethoxychalcones **4** and **5**, pyrazole **10**) [[14,18, 19,51,52](#)] to moderate (i. e., flavokawain **A 2**, benzochalcone **9** and enone **11**) [[18,23,24,45](#)] cytotoxic activity, which could partly explain their toxicity at 100  $\mu$ M. However, the cytometric detection of cell destruction rather than apoptosis induction, occurring rapidly at high concentration of competitors, suggests detergent-like effects deviating from classical inhibition or death pathways.

#### 4. Conclusion

The novel fluorogenic probe **HAB** was found to be non-toxic to *L. amazonensis* promastigotes at 5  $\mu$ M in medium-duration (>1 h) experiments, allowing its use as a cytopermeable, rapidly penetrating vital stain in parasites. Using microscopic imaging, **HAB** was found to distinctly label three subcellular compartments (i. e., ACC, lysosomes and mitochondria) in live promastigotes. A faint blue-emitting dye under its free form, **HAB** undergoes strong bathochromic fluorescence turn-ons in presence of intracellular biological targets [[12](#)]. Consistently, it was detected in the yellow-orange region of the emission spectrum following excitation with blue light in promastigotes, but also in non-infected macrophages and amastigotes ([Figs. S7 and S8, Supporting Information](#)), reminiscent of its behavior in zebrafish larva [[12](#)].

Pharmacologically, **HAB** showed a general ability for the binding



profiling of chalcones and analogues using live-cell flow cytometry. However, it also presented with limitations as a reversible probe for competition studies: firstly, some important antileishmanials of therapeutic interest, such as chalcones **2**, **3** and **5**, could not be profiled using this methodology due to their fast (< 70 min) lysis of up to 82% cells, leading to aberrant assessments of the competitive blockage in surviving cell populations. Attempts to decrease **HAB** concentration - and in turn, that of competitor, while keeping a 1:20 stoichiometry - were unsuccessful due to the cytometric detection limit of 5  $\mu$ M for **HAB** in live *L. amazonensis* promastigotes; secondly, while some exogenous chalcones did act as competitors, blockage values were consistently moderate (ca. 20–30%) even in the case of potent antiparasitic compounds (e. g., chalcones **4** and **7**). Accordingly, none of these competitors could see its action detected at the level of putative affinity organelles using live cell imaging. This behavior suggests that **HAB**, despite its good antipromastigote activity (Table 1), does not feature a sufficiently representative chalconic structure to target canonical binding sites in *Leishmania*. This hypothesis echoes previous observations made in zebrafish neutrophils, where highly relevant bioactive chalcones failed to compete with **HAB** [12].

Current efforts to identify chalcone targets in *Leishmania* parasites rely on "click" chemistry, taking advantage of the covalent bond formed between the inhibitor and the target(s) [7]. While this approach is restricted to chalcones acting irreversibly, it also depends on sequential derivatization steps and is so far incompatible with live-cell fluorogenic imaging [7]. Capitalizing on our study, future efforts to decipher chalcone binding sites in *Leishmania* might consider fluorogenic probes integrating pharmacophoric rings A (i. e., 2'-hydroxy-4',6'-dimethoxyphenyl or 3',4',5'-trimethoxyphenyl) in their structure, to achieve optimal pharmacological specificity. In particular, probes allowing for the precise characterization of chalcone affinity sites in *Leishmania* intramacrophage amastigotes would be invaluable to unravel the mechanisms of action of this chemical series.

Last, it must be emphasized that our probe-mediated strategy of indirect target prospecting could be applied to other chalcone-sensitive parasites of medical importance (e. g., *Plasmodium* and *Trypanosoma*) [53–58].

#### CRediT authorship contribution statement

A. S. B. and S. D. S. O. performed all microscopic imaging. S. P. performed promastigote culture and growth inhibition assays. P-H. C. performed cytometric analysis and data processing. V. M. performed **HAB** spectrophotometric analysis and data processing. M. L. performed synthesis of cpd. **9-11**. P. M. L. processed growth inhibitory assays data. B. R.-B. performed macrophage and amastigote culture. E. P. performed promastigote culture and competition experiments prior to cytometric analysis. R. D. performed synthesis of **HAB** and cpd. **2**, **3**, **6** and **8**, designed and supervised the project, analysed data and wrote the manuscript.

#### Conflict of interest statement

The authors have no interest to declare.

#### Acknowledgements

The authors wish to acknowledge the following contributors: Prof. G. Lewin (BioCIS, Université Paris-Sud 11) for the kind gift of chalcones **4**, **5** and **7**; Dr. P. Leal (Universidade Federal de Santa Catarina) for the generous gift of xanthoxylone, synthetic precursor of flavokawain A **2** and chalcone **3**; Prof. K. Miranda and Prof. F. Gomez (Universidade Federal de Rio de Janeiro) for providing with anti-vacuolar-type proton pyrophosphatase antibodies and for stimulating discussions regarding ACC; Prof. R. Coutinho-Silva (Universidade Federal de Rio de Janeiro) for helping with the promastigote microscopy experiments; Dr J.

Moreira (Owkin) for translating the CNPq scientific proposal into Portuguese. Grant from the Conselho Nacional de Desenvolvimento Científico e Tecnológico, CNPq (401897/2010-9 to R. D.) is acknowledged.

#### Appendix A. Supporting information

Supplementary data associated with this article can be found in the online version at doi:10.1016/j.biopha.2022.112784.

#### References

- [1] J.R. Dimmock, D.W. Elias, M.A. Beazely, N.M. Kandepu, Bioactivities of chalcones, *Curr. Med Chem.* 6 (1999) 1125–1149.
- [2] C. Zhuang, W. Zhang, C. Sheng, W. Zhang, C. Xing, Z. Miao, Chalcone: a privileged structure in medicinal chemistry, *Chem. Rev.* 117 (2017) 7762–7810.
- [3] B. Zhou, C. Xing, Diverse molecular targets for chalcones with varied bioactivities, *Med Chem.* 5 (2015) 388–404.
- [4] C. Karthikeyan, N.S. Moorthy, S. Ramasamy, U. Vanam, E. Manivannan, D. Karunakaran, P. Trivedi, Advances in chalcones with anticancer activities, *Recent Pat. Anticancer Drug Discov.* 10 (2015) 97–115.
- [5] N. Al-Rifai, H. Rucker, S. Amslinger, Opening or closing the lock? When reactivity is the key to biological activity, *Chemistry* 19 (2013) 15384–15395.
- [6] M. Hachet-Haas, K. Balabanian, F. Rohmer, F. Pons, C. Franchet, S. Lecat, K.Y. C. Chow, R. Dagher, P. Gizzi, B. Didier, B. Lagane, E. Kellenberger, D. Bonnet, B. Baleux, J. Haiech, M. Parmentier, N. Frossard, F. Arenzana-Seisdedos, M. Hibert, J.L. Galzi, Small neutralizing molecules to inhibit actions of the chemokine CXCL12, *J. Biol. Chem.* 283 (2008) 23189–23199.
- [7] D.O. Escrivani, R.L. Charlton, M.B. Caruso, G.A. Burle-Caldas, M.P.G. Borsodi, R. B. Zingali, N. Arruda-Costa, M.V. Palmeira-Mello, J.B. de Jesus, A.M.T. Souza, B. Abraham-Vieira, S. Freitag-Pohl, E. Pohl, P.W. Denny, B. Rossi-Bergmann, P. G. Steel, Chalcones identify cTXNPx as a potential antileishmanial drug target, *PLoS Negl. Trop. Dis.* 15 (2021), e0009951.
- [8] M.M. Miranda-Sapla, F. Tomiotto-Pelliassi, J.P. Assolini, A.C.M. Carlotto, B. Bortoleti, M.D. Gonçalves, E.R. Tavares, J. Rodrigues, A.N.C. Simao, L. M. Yamauchi, C.V. Nakamura, W.A. Verri Jr., I.N. Costa, I. Conchon-Costa, W. R. Pavanelli, Trans-Chalcone modulates *Leishmania amazonensis* infection in vitro by Nr2 overexpression affecting iron availability, *Eur. J. Pharmacol.* 853 (2019) 275–288.
- [9] M. Chen, L. Zhai, S.B. Christensen, T.G. Theander, A. Kharazmi, Inhibition of fumarate reductase in *Leishmania major* and *L. donovani* by chalcones, *Antimicrob. Agents Chemother.* 45 (2001) 2023–2029.
- [10] L.D. Chiaradia, P.G. Martins, M.N. Cordeiro, R.V. Guido, G. Ecco, A. D. Andricopulo, R.A. Yunes, J. Vernal, R.J. Nunes, H. Terenzi, Synthesis, biological evaluation, and molecular modeling of chalcone derivatives as potent inhibitors of Mycobacterium tuberculosis protein tyrosine phosphatases (PtpA and PtpB), *J. Med Chem.* 55 (2012) 390–402.
- [11] R. Prajapati, S.H. Seong, S.E. Park, P. Paudel, H.A. Jung, J.S. Choi, Isoliquiritigenin, a potent human monoamine oxidase inhibitor, modulates dopamine D1, D3, and vasopressin V1A receptors, *Sci. Rep.* 11 (2021) 23528.
- [12] E. Colucci-Guyon, A.S. Batista, S.D.S. Oliveira, M. Blaud, I.C. Bellettini, B. S. Marteyn, K. Leblanc, P. Herbomel, R. Duval, Ultraspecific live imaging of the dynamics of zebrafish neutrophil granules by a histopermeable fluorogenic benzochalcone probe, *Chem. Sci.* 10 (2019) 3654–3670.
- [13] L. Zhai, M. Chen, J. Blom, T.G. Theander, S.B. Christensen, A. Kharazmi, The antileishmanial activity of novel oxygenated chalcones and their mechanism of action, *J. Antimicrob. Chemother.* 43 (1999) 793–803.
- [14] E.C. Torres-Santos, D.L. Moreira, M.A.C. Kaplan, M.N. Meirelles, B. Rossi-Bergmann, Selective effect of 2',6'-dihydroxy-4'-methoxychalcone isolated from *Piper aduncum* on *Leishmania amazonensis*, *Antimicrob. Agents Chemother.* 43 (1999) 1234–1241.
- [15] E.C. Torres-Santos, M.I. Sampaio-Santos, F.S. Buckner, K. Yokoyama, M. Gelb, J. A. Urbina, B. Rossi-Bergmann, Altered sterol profile induced in *Leishmania amazonensis* by a natural dihydroxymethoxylated chalcone, *J. Antimicrob. Chemother.* 63 (2009) 469–472.
- [16] O. Kayser, A.F. Kiderlen, In vitro leishmanicidal activity of naturally occurring chalcones, *Phytother. Res.* 15 (2001) 148–152.
- [17] F. Lunardi, M. Guzela, A.T. Rodrigues, R. Correa, I. Eger-Mangrich, M. Steindel, E. C. Grisard, J. Assreuy, J.B. Calixto, A.R. Santos, Trypanocidal and leishmanicidal properties of substitution-containing chalcones, *Antimicrob. Agents Chemother.* 47 (2003) 1449–1451.
- [18] P. Boeck, C.A.B. Falcao, P.C. Leal, R.A. Yunes, V. Cechinel, E.C. Torres-Santos, B. Rossi-Bergmann, Synthesis of chalcone analogues with increased antileishmanial activity, *Bioorg. Med. Chem.* 14 (2006) 1538–1545.
- [19] J. Quintin, J. Desrivot, S. Thoret, P. Le Menez, T. Cresteil, G. Lewin, Synthesis and biological evaluation of a series of tangeretin-derived chalcones, *Bioorg. Med. Chem. Lett.* 19 (2009) 167–169.
- [20] J.C. Aponte, D. Castillo, Y. Estevez, G. Gonzalez, J. Arevalo, G.B. Hammond, M. Sauvain, In vitro and in vivo anti-*Leishmania* activity of polysubstituted synthetic chalcones, *Bioorg. Med. Chem. Lett.* 20 (2010) 100–103.
- [21] M.L. Bello, L.D. Chiaradia, L.R. Dias, L.K. Pacheco, T.R. Stumpf, A. Mascarello, M. Steindel, R.A. Yunes, H.C. Castro, R.J. Nunes, C.R. Rodrigues, Trimethoxychalcone derivatives inhibit growth of *Leishmania braziliensis*: synthesis,

- biological evaluation, molecular modeling and structure-activity relationship (SAR), *Bioorg. Med. Chem.* 19 (2011) 5046–5052.
- [22] M.S. Osman, T.A. Awad, S.W. Shantier, E.A. Garelnabi, W. Osman, R.A. Mothana, F.A. Nasr, R.I. Elhag, Identification of some chalcone analogues as potential antileishmanial agents: an integrated *in vitro* and *in silico* evaluation, *Arab. J. Chem.* 15 (2022) 1–10.
- [23] V. Satam, R.K. Bandi, A.K. Behera, B.K. Mishra, S. Tzou, O. Brockway, B. Babu, M. Zeller, C. Westbrook, S.L. Mooberry, M. Lee, H. Pati, Design, synthesis, and cytotoxicity of novel 3-arylidenedones derived from alicyclic ketones, *Chem. Biol. Drug Des.* 78 (2011) 700–708.
- [24] K.A. Brien, R.K. Bandi, A.K. Behera, B.K. Mishra, P. Majumdar, V. Satam, M. Savagian, S. Tzou, M. Lee, M. Zeller, A.J. Robles, S. Mooberry, H. Pati, M. Lee, Design, synthesis and cytotoxicity of novel chalcone analogs derived from 1-cyclohexylpyrrolidin-2-one and 2,3-dihydrobenzo[f]chromen-1-one, *Arch. Pharm.* 345 (2012) 341–348.
- [25] R. LeBlanc, J. Dickson, T. Brown, M. Stewart, H.N. Pati, D. VanDerveer, H. Arman, J. Harris, W. Pennington, H.L. Holt Jr., M. Lee, Synthesis and cytotoxicity of epoxide and pyrazole analogs of the combretastatins, *Bioorg. Med. Chem.* 13 (2005) 6025–6034.
- [26] Y.J. Oh, Y.H. Seo, A novel chalcone-based molecule, BDP inhibits MDAMB231 triple-negative breast cancer cell growth by suppressing Hsp90 function, *Oncol. Rep.* 38 (2017) 2343–2350.
- [27] J.H. Jeong, Y.J. Oh, T.K. Kwon, Y.H. Seo, Chalcone-templated Hsp90 inhibitors and their effects on gefitinib resistance in non-small cell lung cancer (NSCLC), *Arch. Pharm. Res.* 40 (2017) 96–105.
- [28] C. Chollet, B. Crousse, C. Bories, D. Bonnet-Delpon, P.M. Loiseau, *In vitro* antileishmanial activity of fluoro-artemisinin derivatives against *Leishmania donovani*, *Biomed. Pharmacother.* 62 (2008) 462–465.
- [29] K.A. Mullin, B.J. Foth, S.C. Ilgoutz, J.M. Callaghan, J.L. Zawadzki, G.I. McFadden, M.J. McConville, Regulated degradation of an endoplasmic reticulum membrane protein in a tubular lysosome in *Leishmania mexicana*, *Mol. Biol. Cell* 12 (2001) 2364–2377.
- [30] R.F. Waller, M.J. McConville, Developmental changes in lysosome morphology and function *Leishmania* parasites, *Int. J. Parasitol.* 32 (2002) 1435–1445.
- [31] K. Miranda, R. Docampo, O. Grillo, A. Franzen, M. Attias, A. Vercesi, H. Plattner, J. Hentschel, W. de Souza, Dynamics of polymorphism of acidocalcisomes in *Leishmania* parasites, *Histochem. Cell Biol.* 121 (2004) 407–418.
- [32] S.N. Moreno, R. Docampo, The role of acidocalcisomes in parasitic protists, *J. Eukaryot. Microbiol.* 56 (2009) 208–213.
- [33] F.J. Li, C.Y. He, Acidocalcisome is required for autophagy in *Trypanosoma brucei*, *Autophagy* 10 (2014) 1978–1988.
- [34] S. Besteiro, D. Tonn, L. Tetley, G.H. Coombs, J.C. Mottram, The AP3 adaptor is involved in the transport of membrane proteins to acidocalcisomes of *Leishmania*, *J. Cell Sci.* 121 (2008) 561–570.
- [35] J.E. Vince, D.L. Tull, T. Spurck, M.C. Derby, G.I. McFadden, P.A. Gleeson, S. Gokool, M.J. McConville, *Leishmania* adaptor protein-1 subunits are required for normal lysosome traffic, flagellum biogenesis, lipid homeostasis, and adaptation to temperatures encountered in the mammalian host, *Eukaryot. Cell* 7 (2008) 1256–1267.
- [36] H.J. Lin, P. Herman, J.S. Kang, J.R. Lakowicz, Fluorescence lifetime characterization of novel low-pH probes, *Anal. Biochem.* 294 (2001) 118–125.
- [37] B. Lemieux, M.D. Percival, J.P. Falgouty, Quantitation of the lysosomotropic character of cationic amphiphilic drugs using the fluorescent basic amine Red DND-99, *Anal. Biochem.* 327 (2004) 247–251.
- [38] H.P. Price, L. MacLean, J. Marrison, P.J. O’Toole, D.F. Smith, Validation of a new method for immobilising kinetoplastid parasites for live cell imaging, *Mol. Biochem. Parasitol.* 169 (2010) 66–69.
- [39] R. Docampo, The origin and evolution of the acidocalcisome and its interactions with other organelles, *Mol. Biochem. Parasitol.* 209 (2016) 3–9.
- [40] M. Kobayashi, K. Sato, Mitochondrial behavior and localization in reconstituted oocytes derived from germinal vesicle transfer, *Hum. Cell* 21 (2008) 7–11.
- [41] M. Di Carlo, P. Picone, R. Carrotta, D. Giacomazza, P.L. San, Biagio, Insulin promotes survival of amyloid-beta oligomers neuroblastoma damaged cells via caspase 9 inhibition and Hsp70 upregulation, *J. Biomed. Biotechnol.* 2010 (2010), 147835.
- [42] T. Horinouchi, H. Nakagawa, T. Suzuki, K. Fukuhara, N. Miyata, A novel mitochondria-localizing nitrobenzene derivative as a donor for photo-uncaging of nitric oxide, *Bioorg. Med. Chem. Lett.* 21 (2011) 2000–2002.
- [43] M. Das, S.B. Mukherjee, C. Shaha, Hydrogen peroxide induces apoptosis-like death in *Leishmania donovani* promastigotes, *J. Cell Sci.* 114 (2001) 2461–2469.
- [44] G. van Zandbergen, A. Bollinger, A. Wenzel, S. Kamhawi, R. Voll, M. Klinger, A. Muller, C. Holscher, M. Herrmann, D. Sacks, W. Solbach, T. Laskay, *Leishmania* disease development depends on the presence of apoptotic promastigotes in the virulent inoculum, *Proc. Natl. Acad. Sci. USA* 103 (2006) 13837–13842.
- [45] X.L. Zi, A.R. Simoneau, Flavokawain A, a novel chalcone from kava extract, induces apoptosis in bladder cancer cells by involvement of Bax protein-dependent and mitochondria-dependent apoptotic pathway and suppresses tumor growth in mice, *Cancer Res.* 65 (2005) 3479–3486.
- [46] M.F. Maioral, C.D.N. Bodack, N.M. Stefanos, A. Bigolin, A. Mascarello, L. D. Chiaradia-Delatorre, R.A. Yunes, R.J. Nunes, M.C. Santos-Silva, Cytotoxic effect of a novel naphthylchalcone against multiple cancer cells focusing on hematologic malignancies, *Biochimie* 140 (2017) 48–57.
- [47] V. Tomeckova, P. Perjesi, J. Guzy, J. Kusnir, Z. Chovanova, Z. Chavkova, M. Marekova, Comparison of effect of selected synthetic chalcone analogues on mitochondrial outer membrane determined by fluorescence spectroscopy, *J. Biochem. Biophys. Methods* 61 (2004) 135–141.
- [48] R.A. Duval, R.L. Allmon, J.R. Lever, Indium-labeled macrocyclic conjugates of naltrindole: high-affinity radioligands for *in vivo* studies of peripheral delta opioid receptors, *J. Med. Chem.* 50 (2007) 2144–2156.
- [49] M.C. O’Brien, W.E. Bolton, Comparison of cell viability probes compatible with fixation and permeabilization for combined surface and intracellular staining in flow cytometry, *Cytometry* 19 (1995) 243–255.
- [50] H.R. Dharmaratne, N.P. Nanayakkara, I.A. Khan, Kavalactones from Piper methysticum, and their <sup>13</sup>C NMR spectroscopic analyses, *Phytochemistry* 59 (2002) 429–433.
- [51] A.L. Navarini, L.D. Chiaradia, A. Mascarello, M. Fritzen, R.J. Nunes, R.A. Yunes, T. B. Creczynski-Pasa, Hydroxychalcones induce apoptosis in B16-F10 melanoma cells via GSH and ATP depletion, *Eur. J. Med. Chem.* 44 (2009) 1630–1637.
- [52] H.N. Pati, R. LeBlanc, J. Dickson, M. Stewart, T. Brown, M. Lee, Synthesis and cytotoxic properties of nitro- and aminochalcones, *Med. Chem. Res.* 14 (2005) 19–25.
- [53] J.B. Bertoldo, L.D. Chiaradia-Delatorre, A. Mascarello, P.C. Leal, M.N. Cordeiro, R. J. Nunes, E.S. Sarduy, P.J. Rosenthal, H. Terenzi, Synthetic compounds from an in house library as inhibitors of falcipain-2 from *Plasmodium falciparum*, *J. Enzym. Inhib. Med. Chem.* 30 (2015) 299–307.
- [54] B. Insuasty, J. Ramirez, D. Becerra, C. Echeverry, J. Quiroga, R. Abonia, S. M. Robledo, I.D. Velez, Y. Upegui, J.A. Munoz, V. Ospina, M. Noguera, J. Cobo, An efficient synthesis of new caffeine-based chalcones, pyrazolines and pyrazolo[3,4-b][1,4]diazepines as potential antimalarial, antityrosinomal and antileishmanial agents, *Eur. J. Med. Chem.* 93 (2015) 401–413.
- [55] C.E. Gutteridge, J.V. Vo, C.B. Tillett, J.A. Vigilante, J.R. Dettmer, S.L. Patterson, K. A. Werbovetz, J. Capers, D.A. Nichols, A.K. Bhattacharjee, L. Gerena, Antileishmanial and antimalarial chalcones: synthesis, efficacy and cytotoxicity of pyridinyl and naphthalenyl analogs, *Med. Chem.* 3 (2007) 115–119.
- [56] M. Liu, P. Wilairat, S.L. Croft, A.L. Tan, M.L. Go, Structure-activity relationships of antileishmanial and antimalarial chalcones, *Bioorg. Med. Chem.* 11 (2003) 2729–2738.
- [57] A.A.M. Bortoluzzi, I.V. Staffen, F.W. Banhuk, A. Griebler, P.K. Matos, T.S. Ayala, E. A.A. da Silva, M.H. Sarragiotto, I.T.A. Schuquel, T.C.M. Jorge, R.A. Menolli, Determination of chemical structure and anti-*Trypanosoma cruzi* activity of extracts from the roots of *Lonchocarpus cultratus* (Vell.) A.M.G. Azevedo & H.C. Lima, *Saudi J. Biol. Sci.* 28 (2021) 99–108.
- [58] J.C. Aponte, M. Verastegui, E. Malaga, M. Zimic, M. Quiliano, A.J. Vaisberg, R. H. Gilman, G.B. Hammond, Synthesis, cytotoxicity, and anti-*Trypanosoma cruzi* activity of new chalcones, *J. Med. Chem.* 51 (2008) 6230–6234.